



**Statistical correlations of currents flowing through a proximized quantum dot**G. Michałek \* and B. R. Bułka *Institute of Molecular Physics, Polish Academy of Sciences, ul. M. Smoluchowskiego 17, 60-179 Poznań, Poland*T. Domański  and K. I. Wysokiński *Institute of Physics, M. Curie-Skłodowska University, pl. M. Curie-Skłodowskiej 1, 20-031 Lublin, Poland*

(Received 22 January 2020; revised manuscript received 7 May 2020; accepted 13 May 2020; published 1 June 2020)

Statistical properties of the electron transport flowing through nanostructures are strongly influenced by the interactions, geometry of the system, and/or by type of the external electrodes. These factors affect not only the average current induced in the system but also contribute to fluctuations in the flux of charges and their correlations. Due to possible applications of the hybrid nanosystems, containing one or more superconducting electrodes, a detailed understanding of the flow of charge and its fluctuations seems to be of primary importance. Coulomb repulsion between electrons usually strongly affect the current-current correlation function. In this work we study the correlations in the charge flow through such an interacting quantum dot contacted to one superconducting and two normal electrodes. This setup allows for analysis of the Andreev scattering events in the correlations of currents flowing between external electrodes and, in particular, gives access to cross-correlations between currents to or from different normal electrodes. Our approach relies on the master equation technique, which properly captures the Coulomb interactions. We study the finite-frequency correlations and find the relaxation processes, related to the high-frequency charge and low-frequency polarization fluctuations. The multiterminal structure of single-electron device studied here allows us to analyze a competition between the intra- and interchannel correlations. In the appropriate limit of the interacting quantum dot embedded between two normal electrodes our calculations quantitatively describe the recent experimental data on the frequency-dependent correlations. This shows a promising potential of the method for description of the hybrid systems with superconducting electrode(s).

DOI: [10.1103/PhysRevB.101.235402](https://doi.org/10.1103/PhysRevB.101.235402)**I. INTRODUCTION**

Studies of charge transport through the multiterminal nanostructures with quantum dots are important from both practical and fundamental science points of view. Such systems have been proposed as, e.g., efficient heat to electricity converters [1] and sources of entangled electrons [2] in heterojunctions made of the normal and superconducting electrodes. Ability to control their microscopic parameters, such as the energy levels of quantum dots, interactions between opposite spin electrons, and the coupling of quantum dots to external leads makes such heterostructures very appealing. Furthermore, the character of transport can be changed in such nanostructures from the sequential to ballistic tunneling upon varying the macroscopic parameters, e.g., dot size, resistance of the tunnel junctions, gate voltage and bias, temperature, magnetic field, etc. [3,4]. They are thus important playground for studying many-body phenomena, such as the Kondo effect, competition between the local and nonlocal Andreev reflections, and many others [2,5]. Some of these phenomena might find potential applications in nanoelectronics and

spintronics [6] or become basic building blocks of future quantum computers [7–9].

Tunneling processes through a quantum dot embedded between one superconducting and several normal electrodes can be contributed by a number of different events. Electrons may tunnel between the normal electrodes; we call this process electron transfer (ET). Another possible processes rely either on the direct (D) and crossed (C) Andreev reflections (AR), which are the main subject of our study here. Of special interest for applications are the latter processes (CAR), in which two electrons of the strongly entangled BCS singlet state are scattered into different normal electrodes. Such events have been proposed as a source of the spatially separated entangled electrons for potential use in quantum computing [8]. High efficiency of the Cooper pair splitting can be achieved in the systems with strongly interacting quantum dots and detected by measuring nonlocal differential conductance of the Andreev processes [2,10]. Correlations in the electrical currents have indeed provided evidence for such entanglement [6,11–13].

Besides valuable analysis of the conductances one can get additional information about properties of the system, concerning, e.g., mechanism of transport, statistics of quasiparticles contributing to charge transport, role of the Coulomb interactions, relaxation processes, correlations between

\*grzechal@ifmpan.poznan.pl

currents flowing *via* different transport channels and/or different branches of the device by studying the shot noise, i.e., time-dependent fluctuations in electrical currents caused by the charge quantization [14]. In the systems with noninteracting electrons the Pauli exclusion principle is known to cause the antibunching [15], which manifests itself by reduction of the shot noise (autocorrelations) below the Poissonian value  $S_P = 2eJ$  (where  $J$  is an average current flowing through the system) or by negative cross-correlations in the multiterminal systems [14]. It has been found, however, that correlations between the tunneling electrons can also lead to bunching as evidenced by the super-Poissonian noise [16–18]. In the multiterminal structure the dynamical channel blockade could be responsible for enhancement of the shot noise [19,20] and for the positive cross-correlations [20–22]. Such bunching and antibunching features have been indeed observed experimentally (in the auto- and cross-correlations) by McClure *et al.* [23] and Zhang *et al.* [24] for a device, comprising the double quantum dots that are coupled capacitively. Recent measurements [25] of the correlations of currents flowing through the interacting quantum dot contacted by two normal electrodes have shown the ability of experiments to investigate the fingerprints of interactions and the coherence, this being the main theme of our work. We shall comment on this experiment in Sec. III C. However, our system containing the superconducting electrode allows the study of not only the cross-correlations but also the superconducting coherence of electrons on the frequency-dependent Fano factors and other characteristics.

Dynamical correlations have been also studied in electrical currents of superconducting systems, including chaotic cavities [26,27], planar junctions with direct normal metal-superconductor interfaces [28–37], topological wires [38,39], and quantum dot systems in two- [40–47] or three-terminal (Cooper pair splitter) [48–51] configurations, etc. In particular, it has been shown that positive cross-correlations in hybrid systems are a signature of the high efficiency of Cooper pair splitting [48]. Most of the calculations have so far explored the zero-frequency limit [40,41,43,44,46,49,50] in two-terminal setups [40–46] neglecting the Coulomb interactions [40,42]. The short-time dynamics have been recently addressed by means of factorial cumulants in a metallic single-electron box [52] or employing the waiting-time distribution approach to the case of unidirectional transport, i.e., for very large biases [51,53,54].

In this paper we investigate the noise of three-terminal hybrid system with a quantum dot embedded in Y-shape configuration, between one superconducting and two metallic leads. For this nanostructure we analyze an interplay between the tunneling of normal electrons and the Andreev reflection processes evidenced in the auto- and cross-correlations between tunneling currents and in the corresponding Fano factors. Our considerations go beyond the zero-frequency noise, capturing also finite-frequency contributions due to charge fluctuations between the QD and normal tunnel junctions. We restrict this study to the subgap regime (neglecting relaxation processes by the quasiparticles from outside the pairing gap of superconducting lead), and therefore it is practically valid up to milielectronvolt (infrared frequencies) region. Furthermore, we do not address any short-time coherent oscillations of the

electron pairs between the QD and superconducting reservoir [55]. The zero-frequency noise explored previously in the literature describes total fluctuations, which are rather noisy. Our studies extended onto the finite-frequency range give an insight into the dynamics of electron and hole tunneling processes and their correlations. We are thus able to single out from such a noisy spectrum the relaxation processes contributed by the individual subgap quasiparticles.

Our study is based on the master equation method, reliable for the incoherent tunneling regime  $k_B T \gg \Gamma_{L(R)}$  (where  $\Gamma_{L(R)}$  denotes tunneling rate between QD and the metallic lead). This analysis of frequency-dependent noises for a three-terminal hybrid device with the proximized QD significantly extends earlier studies of two-terminal systems, using the diagrammatic real-time approach and the generalized master equation [44,45]. To facilitate some comparison with former studies and to emphasize the role played by second normal electrode we show also the numerical results obtained for two-terminal N-QD-S system.

The paper is organized as follows. In Sec. II A we introduce the microscopic model, describing the QD strongly coupled to superconducting reservoir and weakly coupled to two metallic electrodes. Next, in Sec. II B, we determine the frequency-dependent current-current correlation functions of the electron and hole charge transport through the in-gap (Andreev) bound states. In Sec. III we present the numerical results, considering the case of small and large biases. We analyze in detail the frequency-dependent Fano factors and current correlations, monitoring contributions from the currents through various Andreev bound states (ABS), which gives insight into internal dynamics of the system. In Sec. III C we discuss the frequency-dependent Fano factors relevant to our model and present their comparison to available experimental data [25] on the quantum dot coupled between two normal terminals. In Sec. IV we summarize the main findings and, in Sec. V, outline some future perspectives related to our study.

## II. MODEL AND METHODOLOGY

### A. Microscopic model

We consider a single-level quantum dot (QD) strongly hybridized with a superconducting lead (S) and weakly coupled between the left (L) and right (R) normal metallic electrodes, as depicted in Fig. 1(a). For simplicity we shall focus on the *superconducting atomic limit*, assuming that a pairing gap  $\Delta$  of the superconducting reservoir is the largest energy scale in our study. This assumption allows us to neglect any single particle tunneling to or from the superconductor, restricting ourselves solely to the subgap tunneling processes. Under such circumstances, an effective Hamiltonian describing the proximized QD takes the BCS-type form [56]

$$H_{\text{eff}} = \epsilon_1 \sum_{\sigma} d_{\sigma}^{\dagger} d_{\sigma} + U n_{\uparrow} n_{\downarrow} - \frac{\Gamma_S}{2} (d_{\uparrow}^{\dagger} d_{\downarrow}^{\dagger} + d_{\downarrow} d_{\uparrow}), \quad (1)$$

where  $\epsilon_1$  is the spin-degenerate energy level,  $d_{\sigma}^{\dagger} (d_{\sigma})$  create (annihilate) an electron with spin  $\sigma = \{\uparrow, \downarrow\}$ ,  $n_{\sigma} \equiv d_{\sigma}^{\dagger} d_{\sigma}$  stands for the number operator, and  $U$  denotes the repulsive Coulomb interaction. The last term in Eq. (1) describes the induced pairing between the opposite spin electrons originating

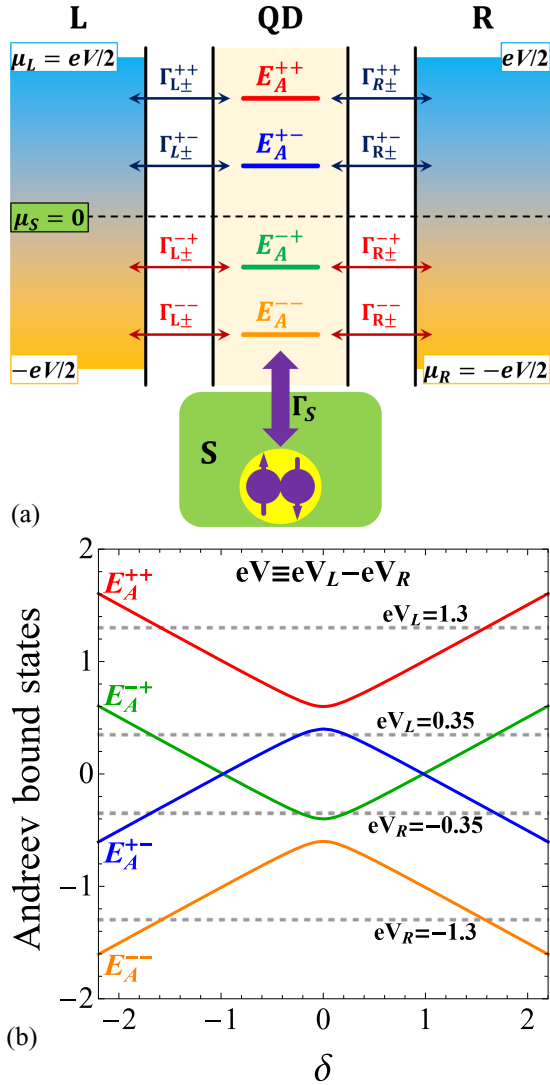


FIG. 1. (a) Schematic view of the hybrid structure, comprising the proximized quantum dot strongly coupled to the superconducting (S) electrode and weakly coupled to the metallic left (L) and right (R) normal leads. Tunneling rates through the Andreev bound states  $E_A^i$  ( $i \in \{ABS\} \equiv \{++, --, +-, -+\}$ ) related to quasiparticle excitations between the even  $\leftrightarrow$  odd eigenstates are indicated by the arrows. For energies above the chemical potential of superconductor ( $\mu_S = 0$ ) the charge carriers are mainly electrons, while below it the holes are dominant. (b) Dependence of ABS on the detuning  $\delta = 2\epsilon_1 + U$  from the half-filled QD. The horizontal dashed lines denote small ( $eV \equiv eV_L - eV_R = 0.7$ ) and large ( $eV = 2.6$ ) bias windows obtained in Sec. III for  $\Gamma_S = 0.2$ , treating the Coulomb potential as the energy unit  $U = 1$ .

from the Cooper pairs leaking onto the QD (superconducting proximity effect). Efficiency of such a process is in the superconducting atomic limit controlled by the coupling  $\Gamma_S$  [49].

The proximized QD, Eq. (1), mixes the empty  $|0\rangle$  with doubly occupied  $|D\rangle \equiv |\uparrow\downarrow\rangle$  configurations. True eigenstates are thus represented by the coherent superpositions  $|- \rangle = \alpha_+|0\rangle + \alpha_-|D\rangle$  and  $|+ \rangle = \alpha_-|0\rangle - \alpha_+|D\rangle$  with the eigenenergies  $\epsilon_{\pm} = \delta/2 \pm \epsilon_A$ , where the BCS coefficients are  $2\alpha_{\pm} = \sqrt{2 \pm \delta/\epsilon_A}$ . For convenience, we have introduced  $2\epsilon_A =$

$\sqrt{\delta^2 + \Gamma_S^2}$  accounting for the energy splitting between  $|+\rangle$  and  $|-\rangle$  states, whereas  $\delta = 2\epsilon_1 + U$  describes detuning between  $|0\rangle$  and  $|D\rangle$  states [44,45,53,57]. Besides these even states  $|\pm\rangle$  there exists also a subspace of the odd (singly occupied) states  $|\uparrow\rangle$  and  $|\downarrow\rangle$  with the degenerate eigenenergy  $\epsilon_1$  (unless a magnetic field is applied).

Charge transport between the normal electrodes via the proximized QD is strictly related to quasiparticle transitions between the even and odd eigenstates. Optimal conditions for the subgap conductance occur when the bias voltage  $V$  is tuned to energy difference between the initial and final state. Such quasiparticle excitation energies (depicted in Fig. 1) define a set of the Andreev bound states [58]  $E_A^{++} \equiv \epsilon_+ - \epsilon_1 = \epsilon_A + U/2$ ,  $E_A^{+-} \equiv \epsilon_- - \epsilon_1 = -\epsilon_A + U/2$ ,  $E_A^{-+} \equiv \epsilon_1 - \epsilon_- = \epsilon_A - U/2$ , and  $E_A^{--} \equiv \epsilon_1 - \epsilon_+ = -\epsilon_A - U/2$ . The gate voltage or  $\delta$  dependence of the Andreev states is shown in Fig. 1(b). Depending on the source-drain voltage  $eV = \mu_L - \mu_R$ , also marked in the figure, two or more Andreev bound states participate in the transport. The chemical potential of the left (right) normal electrode is denoted by  $\mu_L$  ( $\mu_R$ ). We shall consider two situations, corresponding to small ( $eV = 0.7$ ) and large ( $eV = 2.6$ ) bias, respectively.

The metallic leads are represented by the free fermions

$$H_\alpha = \sum_{k,\sigma} (\epsilon_{\alpha k} - \mu_\alpha) c_{\alpha k \sigma}^\dagger c_{\alpha k \sigma}, \quad (2)$$

where  $c_{\alpha k \sigma}^\dagger$  ( $c_{\alpha k \sigma}$ ) creates (annihilates) an itinerant electron with spin  $\sigma = \{\uparrow, \downarrow\}$  and momentum  $k$  in the lead  $\alpha = \{L, R\}$ . Hybridization of the proximized QD, Eq. (1), with both external metallic electrodes is given by

$$H_T = \sum_{\alpha,k,\sigma} (t_\alpha c_{\alpha k \sigma}^\dagger d_\sigma + t_\alpha^* d_\sigma^\dagger c_{\alpha k \sigma}). \quad (3)$$

Since we are interested in the low-energy physics, safely smaller than the superconducting energy gap  $\Delta$ , it is convenient to introduce the tunneling rates  $\Gamma_\alpha$  describing electron and hole transfer between the QD and metallic leads. In the wide-band limit approximation these tunneling rates  $\Gamma_\alpha = 2\pi \sum_k |t_\alpha|^2 \delta(E - \epsilon_{\alpha k}) = 2\pi |t_\alpha|^2 \rho_\alpha$ , where  $\rho_\alpha$  is the density of states in the normal metal lead  $\alpha = \{L, R\}$ , can be approximated by the constant parameters.

## B. Currents and noise

We are interested in dynamical fluctuations of the current from its averaged value,  $\Delta \hat{J}_\alpha(t) \equiv \hat{J}_\alpha(t) - \langle J_\alpha(t) \rangle$ . Definitions of these currents are presented in the Appendix. To describe the current fluctuations in the contact  $\alpha$  and  $\beta$  we use the time correlation function [14]

$$S_{\alpha\beta}(t, t') \equiv \frac{1}{2} \langle \Delta \hat{J}_\alpha(t) \Delta \hat{J}_\beta(t') + \Delta \hat{J}_\beta(t') \Delta \hat{J}_\alpha(t) \rangle. \quad (4)$$

For the case with time-independent external fields the correlation function is a function of  $\tau = t' - t$ , and its Fourier transform can be expressed as

$$S_{\alpha\beta}(\omega) = 2 \int_{-\infty}^{\infty} d\tau e^{i\omega\tau} S_{\alpha\beta}(\tau), \quad (5)$$

which is dubbed *noise power*.

To determine the current-current correlation functions for the considered hybrid system we use the generation-recombination approach [59] and the method developed for spinless electron noise in a single electron transistor [60], extending it in our case to the multichannel and multicharge tunneling processes. According to this procedure, the correlation function between the currents flowing through  $\alpha$ th and  $\beta$ th junctions can be expressed as

$$S_{\alpha\beta}(\omega) = \sum_{i,j \in \{ABS\}} S_{\alpha\beta}^{i,j}(\omega). \quad (6)$$

$$S_{\alpha\beta}^{i,j}(\omega) = \pm 2e^2 \sum_{m,n} \left[ \sum_{\substack{m'>m \\ m''<m}} (M_{m'm}^{\alpha,i} - M_{m''m}^{\alpha,i}) G_{mn}(\omega) \sum_{\substack{n'>n \\ n''<n}} (M_{nn'}^{\beta,j} p_{n'}^0 - M_{nn''}^{\beta,j} p_{n''}^0) \right. \\ \left. + \sum_{\substack{m'>m \\ m''<m}} (M_{m'm}^{\beta,j} - M_{m''m}^{\beta,j}) G_{mn}(-\omega) \sum_{\substack{n'>n \\ n''<n}} (M_{nn'}^{\alpha,i} p_{n'}^0 - M_{nn''}^{\alpha,i} p_{n''}^0) \right], \quad (8)$$

where  $\mathbf{M}$  is the matrix entering the master equation (A1) describing the system studied here, and  $G_{mn}(\omega) = (i\omega\mathbf{1} - \mathbf{M})_{mn}^{-1} - p_m^0/i\omega$  is the matrix Green's function of the proximized QD. The parameters  $p_n^0$  are the stationary solutions of the master equation. We refer the reader to the Appendix for a detailed discussion of the functions  $M_{mn}^{\alpha,i}$ , which are the off-diagonal elements of the matrix  $\mathbf{M}$  related to the currents contributed through the  $\alpha$ th junction via the  $i$ th Andreev bound state. The sign (+) refers to the cross-correlation function between the currents from different (L and R) leads, while the opposite sign (−) corresponds to the autocorrelations between the currents from the same lead.

We have performed numerical calculations for the diagonalized master equation. Such an approximation is valid for the strongly proximized QD ( $\Gamma_S \gg \Gamma_{L(R)}$ ), when the subgap Andreev bound states are long lived. We have checked that in the absence of the Coulomb interactions the effective currents calculated from the diagonalized master equation (DME) are quantitatively consistent with the currents of coherent transport determined within the nonequilibrium Green function technique [61] in the limit  $\Gamma_{L(R)} \ll k_B T, \Gamma_S$ . In the next section we present the main results of our numerical calculations obtained for the aforementioned currents and their correlations, respectively.

### III. RESULTS

Deep in the superconducting gap the charge can be transmitted through our hybrid setup by one of three possible mechanisms: (1) single electron transfer (ET) between the metallic electrodes, (2) direct Andreev reflection (DAR) when incoming electrons from the metallic lead are converted into the on-dot pairs reflecting holes back to the same normal lead, and (3) crossed Andreev reflection (CAR), when holes are reflected to the opposite normal lead. The last case corresponds obviously to the nonlocal transport processes.

Here we specified the contributions  $S_{\alpha\beta}^{i,j}(\omega)$  to the correlation function originating from the currents  $\hat{J}_\alpha^i$  and  $\hat{J}_\beta^j$  through various ABS ( $i, j \in \{++, +-, -+, --\}$ ). They are formally defined by

$$S_{\alpha\beta}^{i,j}(\omega) = \delta_{\alpha\beta} \delta_{ij} S_\alpha^{Sch,i} + S_{\alpha\beta}^{c,i,j}(\omega), \quad (7)$$

where  $S_\alpha^{Sch,i} = 2e(I_{\alpha+}^i + I_{\alpha-}^i)$  is the high-frequency  $\omega \rightarrow \infty$  limit of the shot noise, dubbed the Schottky noise. The Schottky term corresponds to the classical uncorrelated Poissonian transitions. The frequency-dependent part is given by

In what follows we analyze the current correlations obtained for the symmetric case, when the applied voltage  $V$  equally detunes the chemical potential of the left ( $eV_L = eV/2$ ) and right ( $eV_R = -eV/2$ ) metallic leads. The superconducting reservoir is assumed to be grounded  $\mu_S = 0$ . Under such circumstances the contribution from the crossed Andreev reflections to the net current vanishes. Furthermore,  $J_R = -J_L$  and  $J_S \equiv 0$ , therefore the superconducting electrode can be regarded as a floating voltage probe [62]. Zero-frequency current fluctuations in the ballistic regime of the normal multiterminal hybrid structures (without floating superconductor) are characterized by the positive correlations [28]. It has been pointed out, however, that in the metal-superconductor-metal junctions such behavior cannot be caused by the Cooper pair splitting [31,33]. In contrast, we predict here the current fluctuations in the tunneling regime, where a positive sign of the cross-correlations originates from the CAR processes [33].

For comparison with the previous studies, we also include the results obtained for the N-QD-S system (dashed lines in Figs 2–4) determined by imposing  $\Gamma_R = 0$ .

#### A. Current correlations in the small bias regime

We start by considering the charge transport driven by a small bias  $V$  which activates only two (the most inner) Andreev bound states. In Fig. 2 we display the total current  $J_L$  and its components. For a small bias voltage [Fig. 2(a)], the currents appear only for  $eV_L > E_A^{+-}, E_A^{-+}$  while in the remaining regions (corresponding to the doubly occupied and empty states as well as the Coulomb blockade) the currents vanish exponentially. Furthermore,  $J_L^{+-}$  and  $J_L^{-+}$  are asymmetric with respect to the electron-hole symmetry ( $\delta = 0$ ). Both currents originate predominantly from the ET processes over the entire conducting region, whereas DAR processes are enhanced only close to the Coulomb blockade (CB) region. For comparison, we have also plotted the currents obtained for the two-terminal N-QD-S nanostructure, setting  $\Gamma_R = 0$



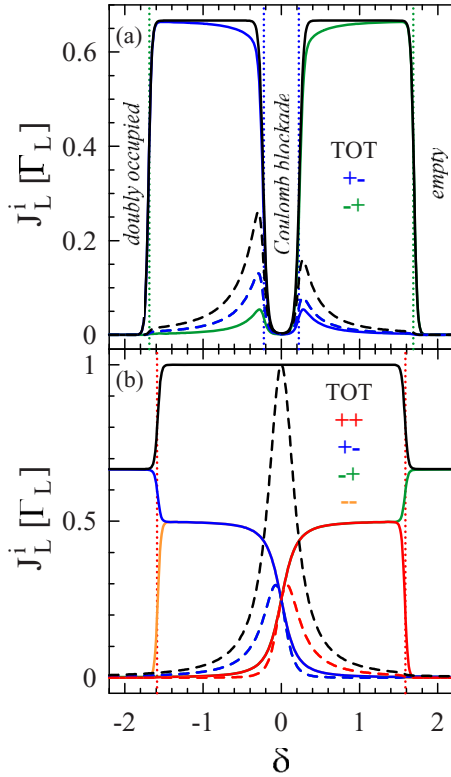


FIG. 2. The charge current  $J_L$  (black) and its components  $J_L^{++}$  (red),  $J_L^{+-}$  (blue),  $J_L^{-+}$  (green), and  $J_L^{--}$  (orange) versus the gate voltage  $\delta$  obtained for the three-terminal setup with symmetric couplings  $\Gamma_R = \Gamma_L$ , assuming the symmetrical bias with (a) small  $eV_L = 0.35 = -eV_R$  and with (b) large  $eV_L = 1.3 = -eV_R$ . For comparison we also plot  $J_L$  and its components for the two-terminal N-QD-S case, imposing  $\Gamma_R = 0$  (dashed curves). The dotted vertical lines indicate positions of the Andreev bound states  $E_A^{++}$  (red),  $E_A^{+-}$  (blue), and  $E_A^{-+}$  (green). Numerical computations have been done for  $\Gamma_S = 0.2$ ,  $\Gamma_R = \Gamma_L = 0.002$ , and  $k_B T = 0.01$ .

(see dashed lines), where only DAR processes are present. In this case the currents  $J_L^{+-}$  and  $J_L^{-+}$  are nearly identical and reveal only a small asymmetry with respect to  $\delta = 0$  caused by the bias asymmetry. In the Coulomb blockade region these currents are much larger than in the three-terminal system, because in the latter case the DAR processes are suppressed by the ET tunneling.

In Fig. 3 we present the zero-frequency current-current correlations. In particular, we display the zero-frequency Fano factor  $F_L = S_{LL}/2eJ_L$  of L-QD junction [Fig. 3(a)], the autocorrelation function  $S_{LL}$  [Fig. 3(b)], the cross-correlation function  $S_{LR}$  between different metallic leads [Fig. 3(c)], and the autocorrelation function  $S_{SS}$  of S-QD junction [Fig. 3(d)]. We can notice that all these quantities are symmetric with respect to  $\delta = 0$ . In the doubly occupied and in the empty state regime the zero-frequency Fano factor  $F_L \approx 1$ , indicating that such current noise is a prevalent feature in the uncorrelated Poissonian tunneling of electrons. In the conducting regime the zero-frequency Fano factor diminishes  $F_L < 1$  (i.e., the noise has sub-Poissonian character), which is a signature of negative correlation of the tunneling events. For the half-filled QD ( $\delta = 0$ ) case, the zero-frequency Fano factor  $F_L \approx 2$  due

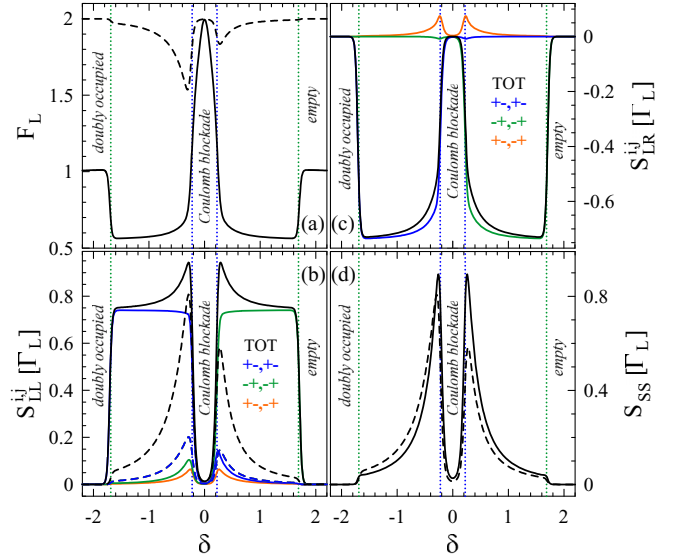


FIG. 3. The zero-frequency current correlations: (a) Fano factor  $F_L$  for L-QD junction; (b) autocorrelation function  $S_{LL}$  (black curve) and its constituents corresponding to various bound states (color curves); (c) cross-correlation function  $S_{LR}$  (black curve) and its components; and (d) autocorrelation function for superconducting electrode versus the gate voltage  $\delta$  obtained for small voltages  $eV_L = 0.35 = -eV_R$  assuming the symmetric couplings  $\Gamma_R = \Gamma_L$ . Dashed curves display results for the two-terminal N-QD-S case ( $\Gamma_R = 0$ ) and dotted vertical lines indicate positions of the Andreev bound states  $E_A^{+-}$  (blue) and  $E_A^{-+}$  (green). Other parameters are the same as those in Fig. 2.

to uncorrelated tunneling of the Cooper pairs. The system is then in the Coulomb blockade, where single-electron tunneling is suppressed at the expense of the AR processes [61–63].

To get more insight into the dynamics and correlations between various tunneling processes we have also calculated the frequency-dependent noise. In the regime of unidirectional transport (i.e., for  $eV_L$  larger than  $E_A^{+-}$  and  $E_A^{-+}$ ) one can derive some analytical results. Let us underline that in the case of small bias only two (the most inner) Andreev bound states  $E_A^{+-}$  and  $E_A^{-+}$  participate in the subgap charge transport. The frequency-dependent Fano factor is then expressed by

$$F_L(\omega) = 1 - \frac{4(\alpha_-^4 + \alpha_+^4)\Gamma_L^2}{9\Gamma_L^2 + \omega^2} + \frac{10\alpha_-^2\alpha_+^2\Gamma_L^2}{9\Gamma_L^2 + \omega^2}. \quad (9)$$

The first (frequency-dependent) term comes from the autocorrelation tunneling processes through the Andreev bound states, for which the correlation functions are given by

$$S_{LL}^{+-,+-}(\omega) = \frac{4}{3}e^2\alpha_-^2\Gamma_L \left(1 - \frac{4\alpha_-^2\Gamma_L^2}{9\Gamma_L^2 + \omega^2}\right), \quad (10)$$

$$S_{LL}^{-+,-+}(\omega) = \frac{4}{3}e^2\alpha_+^2\Gamma_L \left(1 - \frac{4\alpha_+^2\Gamma_L^2}{9\Gamma_L^2 + \omega^2}\right). \quad (11)$$

The second frequency-dependent term [appearing in Eq. (9)] comes from the electron-hole correlations

$$S_{LL}^{+-,-+}(\omega) = \frac{20}{3}e^2\frac{\alpha_-^2\alpha_+^2\Gamma_L^3}{9\Gamma_L^2 + \omega^2}. \quad (12)$$

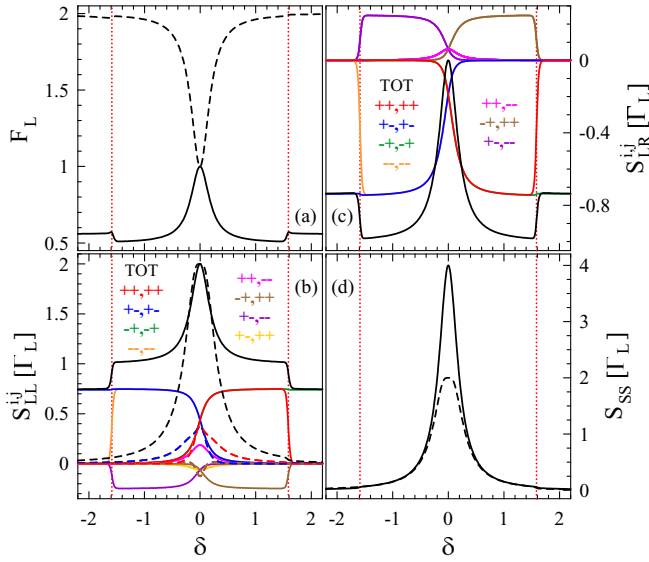


FIG. 4. The zero-frequency current correlation functions: (a) Fano factor  $F_L$  of L-QD junction; (b) autocorrelation function  $S_{LL}$  (black curve) and its contributions through various bound states (color curves); (c) cross-correlation function  $S_{LR}$  (black curve) and its components, where note that  $S_{LR}^{+-,++}(\omega=0) = S_{LR}^{+,-,+}(\omega=0)$ ; and (d) autocorrelation function for  $S$  electrode plotted as a function of gate voltage  $\delta$  for moderate applied voltages  $eV_L = 1.3 = -eV_R$  assuming the symmetric couplings  $\Gamma_R = \Gamma_L$ . For comparison the results for the two-terminal case (N-QD-S) with  $\Gamma_R = 0$  are shown by the dashed curves. Dotted red vertical lines denote positions of the Andreev bound state  $E_A^{++}$ . Other parameters are the same as those in Fig. 2.

Figure 3(b) displays the zero-frequency correlation function  $S_{LL}$  and presents its components  $S_{LL}^{+-,+}$  and  $S_{LL}^{-,+}$  obtained for  $|\delta| < 1$  in the electron and hole transport through the Andreev bound states  $E_A^{++}$  and  $E_A^{-,+}$ . We also present  $S_{LL}^{+-,+}$  describing interlevel correlations between the electron and hole tunneling events. In the conducting regime the main contribution to  $S_{LL}$  comes from  $S_{LL}^{+-,+}$  and  $S_{LL}^{-,+}$ , which reduce the zero-frequency Fano factor  $F \rightarrow 5/9$  in the extreme particle-hole asymmetry case (i.e., a large  $|\delta|$  limit). Notice that such reduction of the zero-frequency Fano factor is smaller than in the N-QD-N system [14,18], where  $F = 1/2$ . This also follows from Eq. (39) below for  $\omega = 0$  and  $\Gamma_R = \Gamma_L$ . Upon approaching the CB region we observe an enhancement of  $S_{LL}$  due to activation of the interlevel correlations  $S_{LL}^{+-,+}$  (orange curve) corresponding to the DAR processes on the L-QD interface. In the Coulomb blockade regime the current  $J_L$  is exponentially suppressed and the corresponding frequency-dependent Fano factor

$$F_L(\omega) = 1 + 2\alpha_-^2 - \frac{32\alpha_-^4\Gamma_L^2}{16\Gamma_L^2 + \omega^2} + \frac{32\alpha_-^2\alpha_+^2\Gamma_L^2}{16\Gamma_L^2 + \omega^2}. \quad (13)$$

The Schottky term is here enhanced by backscattering processes. The first and the second frequency-dependent terms refer to the autocorrelations and interlevel correlations, respectively. Right in a middle of the Coulomb blockade the frequency-dependent terms cancel each other, and  $F_L(\omega = 0) = 2$  (due to backscattering).

Let us notice that in the two-terminal N-QD-S case, the frequency-dependent Fano factor for the conducting regime is given by

$$F_{2t}(\omega) = 1 - \frac{4\alpha_-^2\alpha_+^2\Gamma_L^2}{(\alpha_-^2 + 2\alpha_+^2)\Gamma_L^2 + \omega^2} + \frac{(\alpha_-^4 + 4\alpha_+^4)\Gamma_L^2}{(\alpha_-^2 + 2\alpha_+^2)\Gamma_L^2 + \omega^2}. \quad (14)$$

The second frequency-dependent term [appearing in Eq. (14)] corresponds to the interlevel correlations which is positive and has a dominant contribution. Thereby  $F_{2t}(\omega = 0) > 1$  and the noise has super-Poissonian character. It is always larger than in the three-terminal case; compare the solid and dashed curves in Fig. 3(a). In the Coulomb blockade regime the current and the noise are exponentially suppressed, but the frequency-dependent Fano factor is finite:

$$F_{2t}(\omega) = 1 + \frac{\alpha_-^2}{\alpha_+^2} - \frac{4\alpha_-^2\Gamma_L^2}{\alpha_+^2(4\Gamma_L^2 + \omega^2)} + \frac{4\Gamma_L^2}{4\Gamma_L^2 + \omega^2}. \quad (15)$$

One can see that interlevel correlations are responsible for the super-Poissonian noise; compare with Eq. (13). The positive correlations have been also found for multilevel QD coupled to the normal leads, where the super-Poissonian noise is driven by the interchannel Coulomb blockade [17]. In the regime of the doubly occupied configuration, for the Coulomb blockade and for the empty state  $F_L = 2$  due to uncorrelated jumps of the Cooper pairs to or from the proximized QD. In the conducting regime the dynamical fluctuations between DAR processes induce the negative correlations, and one hence observes a reduction of  $F_L$ .

Figure 3(c) presents the zero-frequency cross-correlation function  $S_{LR}$  between the different metallic leads. Let us remark that in N-QD-N structures the charge conservation rule implies the relation  $S_{LL} = -S_{LR}$  fulfilled at  $\omega = 0$  [14]. The function  $S_{LR}$  is negative for the entire range of the gate voltage  $\delta$ . Far from the Coulomb blockade  $S_{LR} \approx -S_{LL}$  so the components  $S_{LR}^{+-,+}$  and  $S_{LR}^{-,+}$  become dominant because of correlations originating from the ET tunneling processes through metallic junction (see, e.g., Ref. [28]). For the unidirectional transport one can obtain the analytical expression for the frequency-dependent cross-correlation function. For the small bias voltage the transfer rates:  $\Gamma_{L+}^{+-} = \alpha_-^2\Gamma_L$ ,  $\Gamma_{L+}^{-,+} = \alpha_+^2\Gamma_L$ ,  $\Gamma_{R-}^{-,+} = \alpha_+^2\Gamma_R$ ,  $\Gamma_{R-}^{+-} = \alpha_-^2\Gamma_R$ ,  $\Gamma_{L-}^{+-} = \Gamma_{L-}^{-,+} = \Gamma_{R+}^{+-} = \Gamma_{R+}^{-,+} = 0$ ,

$$S_{LR} = -\frac{4e^2}{3} \frac{(5\alpha_+^4 + 5\alpha_-^4 - 8\alpha_-^2\alpha_+^2)\Gamma_L^3}{9\Gamma_L^2 + \omega^2}, \quad (16)$$

with its components

$$S_{LR}^{+-,+}(\omega) = -\frac{20}{3} e^2 \frac{\alpha_-^4\Gamma_L^3}{9\Gamma_L^2 + \omega^2}, \quad (17)$$

$$S_{LR}^{-,+}(\omega) = -\frac{20}{3} e^2 \frac{\alpha_+^4\Gamma_L^3}{9\Gamma_L^2 + \omega^2}, \quad (18)$$

$$S_{LR}^{+-,+}(\omega) = \frac{16}{3} e^2 \frac{\alpha_-^2\alpha_+^2\Gamma_L^3}{9\Gamma_L^2 + \omega^2}. \quad (19)$$

In the case considered here the superconducting electrode plays a crucial role, especially close to the Coulomb blockade

region where the Andreev reflections become important; see Fig. 3(c). The interlevel cross-correlation function  $S_{LR}^{+-,+}$  is positive and then becomes dominant. This is a fingerprint of the correlations between CAR processes [28].

Since we have determined  $S_{LL} = S_{RR}$  and  $S_{LR}$  at  $\omega = 0$ , we can get the correlation function  $S_{SS} = S_{LL} + 2S_{LR} + S_{RR}$  describing correlations in the Cooper pair flow through S-QD interface. As could be expected,  $S_{SS}$  is enhanced close the Coulomb blockade region. The direct and crossed Andreev reflection processes contribute equally to the correlation function  $S_{SS}$  in the symmetric configuration. Notice that the net current  $J_S = 0$  but the corresponding noise  $S_{SS}$  is large. Its value exceeds the ET contribution in  $S_{LL}$ ; compare with the blue and green curves in Fig. 3(b).

### B. Current correlations for large bias

Now let us consider the case of large bias voltage  $eV_L = 1.3 = -eV_R$ , when all the Andreev bound states participate in the subgap transport; see Fig. 1(b). The total current and its components are presented in Fig. 2(b) in a moderate gate voltage range (for larger  $|\delta|$  the QD is in either the double occupied or the empty state and therefore the nanostructure becomes insulating). In the  $|\delta| < E_A^{++}$  energy region one finds the current  $J_L = e\Gamma_L$ , and it is a sum of the appropriate electron and hole currents (see Fig. 1), obeying the conditions  $J_L^- = J_L^+ = e\alpha_+^2\Gamma_L/2$  and  $J_L^- = J_L^- = e\alpha_-^2\Gamma_L/2$ . Since we consider the symmetric case with  $\Gamma_L = \Gamma_R$  the partial currents on R-QD junction are  $J_R^+ = J_R^+ = -e\alpha_+^2\Gamma_L/2$  and  $J_R^- = J_R^- = -e\alpha_-^2\Gamma_L/2$ . This means the absence of any charge accumulation on the Andreev bound states.

The current  $J_L$  shows a steplike behavior, with large plateau for  $|\delta| < E_A^{++}$ . For large  $|\delta|$  the total current is dominated by the ET processes. For  $\delta = 0$  one finds that all electron and hole currents  $J_L^i$  have the same amplitude, which indicates that DAR and ET processes equally participate in  $J_L$ . When  $|\delta| > E_A^{++}$  the ET processes are seen only in  $J_L^{+-}$  for  $\delta < 0$  or  $J_L^{++}$  for  $\delta > 0$ . At  $\delta = -E_A^{++}$  ( $\delta = E_A^{++}$ ) the new transport channel opens (closes), therefore one observes an enhancement (a suppression) of the current  $J_L^{--}$  ( $J_L^{++}$ ) responsible for an enhancement (a suppression) of  $J_L$ . One can also find that  $J_L^-(\delta) = J_L^+(\delta)$  as well as  $J_L^-(\delta) = J_L^+(\delta)$ , which is caused by the electron-hole symmetry. For comparison, in the two-terminal case, one observes the large peak (centered at  $\delta = 0$ ) of  $J_L$  due to DAR processes.

Let us analyze the results presented in Fig. 4 for the zero-frequency Fano factor  $F_L$  and the current correlation functions  $S_{LL}$ ,  $S_{LR}$ , and  $S_{SS}$  at  $\omega = 0$ . One can notice that the noise has sub-Poissonian character, with  $F_L < 1$ , in the entire conducting range. The zero-frequency Fano factor is suppressed down to 1/2 (for large  $|\delta| > E_{++}$ ) due to the negative correlation in ET tunneling processes. In the center of the plot, for  $|\delta| \rightarrow 0$ , we observe enhancement of the zero-frequency Fano factor caused by DAR processes. The interchannel correlations become relevant, therefore  $F_L \rightarrow 1$ . We also performed the frequency-dependent calculations of the current correlations in the unidirectional transport regime. The frequency-dependent Fano factor can be expressed as

$$F_L(\omega) = 1 - \frac{2(\alpha_-^2 - \alpha_+^2)^2\Gamma_L^2}{4\Gamma_L^2 + \omega^2}. \quad (20)$$

This result differs from that one, corresponding to the two-terminal N-QD-S case,

$$F_{2t}(\omega) = 1 + \frac{(\alpha_-^2 - \alpha_+^2)^2\Gamma_L^2}{\Gamma_L^2 + \omega^2}, \quad (21)$$

where the noise is super-Poissonian [compare the solid and dashed curves in Fig. 4(a)]. The same result has been obtained using the diagrammatic real-time approach by Droste *et al.* [45] for the low-frequency-dependent noise. It is also consistent with earlier studies by Braggio *et al.* [44] who used the full counting statistics technique for the zero-frequency shot noise. The derivation of the current correlations and relaxation processes for the two-terminal case is outlined in the Supplemental Material [68].

Figure 4(b) shows various components of the correlation function  $S_{LL}$ . The frequency-dependent analysis of tunneling events shows important role of the intra- and interchannel dynamics. Autocorrelation functions for electrons and holes can be written as

$$\begin{aligned} S_{LL}^{++,++}(\omega) &= S_{LL}^{+-,+}(\omega) \\ &= e^2\alpha_+^2\Gamma_L \left(1 - \frac{4\alpha_+^2\Gamma_L^2}{16\Gamma_L^2 + \omega^2}\right), \end{aligned} \quad (22)$$

$$\begin{aligned} S_{LL}^{--,--}(\omega) &= S_{LL}^{+-,+}(\omega) \\ &= e^2\alpha_-^2\Gamma_L \left(1 - \frac{4\alpha_-^2\Gamma_L^2}{16\Gamma_L^2 + \omega^2}\right). \end{aligned} \quad (23)$$

The interlevel correlations between electron or hole tunneling processes are expressed by

$$S_{LL}^{+-,--}(\omega) = -\frac{2e^2\alpha_+^4\Gamma_L^3}{4\Gamma_L^2 + \omega^2} + \frac{4e^2\alpha_-^4\Gamma_L^3}{16\Gamma_L^2 + \omega^2}, \quad (24)$$

$$S_{LL}^{--,++}(\omega) = -\frac{2e^2\alpha_-^4\Gamma_L^3}{4\Gamma_L^2 + \omega^2} + \frac{4e^2\alpha_+^4\Gamma_L^3}{16\Gamma_L^2 + \omega^2}. \quad (25)$$

Notice that in these expressions the first frequency term is negative, and it dominates at small frequencies, leading to sub-Poissonian noise. The electron-hole correlation functions between different channels are given by

$$\begin{aligned} S_{LL}^{++,--}(\omega) &= S_{LL}^{+-,+}(\omega) \\ &= \frac{2e^2\alpha_-^2\alpha_+^2\Gamma_L^3}{4\Gamma_L^2 + \omega^2} + \frac{4e^2\alpha_-^2\alpha_+^2\Gamma_L^3}{16\Gamma_L^2 + \omega^2}, \end{aligned} \quad (26)$$

$$S_{LL}^{--,++}(\omega) = S_{LL}^{+-,+}(\omega) = -\frac{4e^2\alpha_-^2\alpha_+^2\Gamma_L^3}{16\Gamma_L^2 + \omega^2}. \quad (27)$$

The sum of all these components, Eqs. (22)–(27), leads to

$$S_{LL}(\omega) = 2e^2\Gamma_L \left[1 - \frac{2(\alpha_-^2 - \alpha_+^2)^2\Gamma_L^2}{4\Gamma_L^2 + \omega^2}\right], \quad (28)$$

where only the low-frequency fluctuations play a role whereas the contributions (negative and positive) of the high-frequency fluctuations cancel themselves.

Denominators of the frequency-dependent terms appearing in the correlation functions [Eqs. (22)–(28)] describe a relaxation driven by the generation-recombination processes [59]. For any local quantity described by an operator  $\hat{X}$  its

dynamical fluctuation can be expressed by

$$S_{XX}(\omega) = 4 \sum_{m,n} X_m G_{mn}(\omega) X_n P_n^0, \quad (29)$$

where  $X_m$  is an eigenvalue of  $\hat{X}$ . Equations (8) and (29) are consistent with the quantum regression theorem, which predicts that the equation of motion for the statistically averaged operator implies the same equation for the time-correlation function of this operator [64,65]. Following Ref. [19] one can define operators for a local charge  $\hat{N} = \hat{n}_+ + \hat{n}_-$  and polarization  $\hat{P} = \hat{n}_+ - \hat{n}_-$ , where  $\hat{n}_+$  and  $\hat{n}_-$  are the number operators for the state  $|+\rangle$  and  $|-\rangle$ , respectively. In the case of large bias (considered here) the corresponding charge (polarization) noises are given by

$$S_{NN} = \frac{4\Gamma_L}{16\Gamma_L^2 + \omega^2}, \quad (30)$$

$$S_{PP} = \frac{4\Gamma_L}{4\Gamma_L^2 + \omega^2}. \quad (31)$$

Thus, one can identify the terms with the relaxation rate  $1/\tau_{\text{rel}}^{\text{ch}} = 4\Gamma_L$  in the current noise as corresponding to the high-frequency charge fluctuations on the Andreev bound states, while the terms with  $1/\tau_{\text{rel}}^{\text{pol}} = 2\Gamma_L$  describe the low-frequency polarization fluctuations [17,19,20].

Since we focus on the symmetric situation, the polarization fluctuations occur only in the total current noise  $S_{LL}(\omega)$ , Eq. (28). When the symmetry was broken, for  $\Gamma_L \neq \Gamma_R$  or for an asymmetric bias voltage, the displacement currents [66,67] as well as the accumulated charge [18] could substantially affect the current noise, amplifying the frequency-dependent Fano factor. In the asymmetric case  $\Gamma_R \neq \Gamma_L$  the formulas are more complicated, but for completeness and future reference we present them in the Supplemental Material [68].

Figure 4(c) presents the zero-frequency cross-correlation function  $S_{LR}$  and its components between the metallic leads. This quantity is negative, indicating that ET tunneling processes and their correlations are dominant. At the electron-hole symmetry point,  $\delta = 0$ , where the Andreev scatterings become important,  $S_{LR}$  tends to zero. This means that inter-electrode tunneling events are uncorrelated, i.e., Poissonian. The frequency analysis of the current correlation gives

$$S_{LR}(\omega) = -\frac{4e^2(\alpha_-^2 - \alpha_+^2)^2\Gamma_L^3}{4\Gamma_L^2 + \omega^2} \quad (32)$$

with the following components:

$$\begin{aligned} S_{LR}^{++,+}(\omega) &= S_{LR}^{-+,-}(\omega) \\ &= -\frac{2e^2\alpha_+^4\Gamma_L^3}{4\Gamma_L^2 + \omega^2} - \frac{4e^2\alpha_+^4\Gamma_L^3}{16\Gamma_L^2 + \omega^2}, \end{aligned} \quad (33)$$

$$\begin{aligned} S_{LR}^{--,-}(\omega) &= S_{LR}^{+,-,+}(\omega) \\ &= -\frac{2e^2\alpha_-^4\Gamma_L^3}{4\Gamma_L^2 + \omega^2} - \frac{4e^2\alpha_-^4\Gamma_L^3}{16\Gamma_L^2 + \omega^2}, \end{aligned} \quad (34)$$

$$S_{LR}^{-+,+}(\omega) = \frac{4e^2\alpha_+^4\Gamma_L^3}{16\Gamma_L^2 + \omega^2}, \quad (35)$$

$$S_{LR}^{+,-,-}(\omega) = \frac{4e^2\alpha_-^4\Gamma_L^3}{16\Gamma_L^2 + \omega^2}, \quad (36)$$

$$S_{LR}^{++,-}(\omega) = S_{LR}^{-+,-}(\omega) = \frac{4e^2\alpha_+^2\alpha_-^2\Gamma_L^3}{16\Gamma_L^2 + \omega^2}, \quad (37)$$

$$\begin{aligned} S_{LR}^{--,+}(\omega) &= S_{LR}^{+,-,-}(\omega) \\ &= \frac{2e^2\alpha_-^2\alpha_+^2\Gamma_L^3}{4\Gamma_L^2 + \omega^2} - \frac{4e^2\alpha_-^2\alpha_+^2\Gamma_L^3}{16\Gamma_L^2 + \omega^2}. \end{aligned} \quad (38)$$

Notice that  $S_{LR}^{+,-,+}(\omega) = S_{LR}^{-+,-}(\omega)$  [presented in Eq. (38)] describes the electron-hole correlation between the different Andreev bound states, and it is responsible for suppressing  $S_{LR}(\omega = 0) \rightarrow 0$  in the limit  $\delta = 0$ .

In analogy to the previous discussion, we observe that autocorrelation of the  $J_{SS}$  currents in the S-QD junction of the three-terminal system is strongly enhanced at  $\delta = 0$ , as displayed in Fig. 4(d). This is caused by the frequency-dependent part, which is negative and vanishes at  $\delta = 0$ ; see Eq. (28). Its value is equal to the Schottky noise and is twice as large as in two-terminal N-QD-S case; see the dashed curve in Fig. 4(d). This is the result of the aforementioned lack of correlation between electron tunneling through both normal tunnel junctions, therefore the noise simplifies to  $S_{SS}(0) = 2S_{LL}(0) = 4e^2\Gamma_L = 4eJ_L$ .

### C. Frequency dependence of the Fano factors: Experimental consequences

Till now we have been discussing the frequency dependence of the currents and their fluctuations in the three-terminal system with one of the terminals being a superconductor. To our knowledge there are no experimental data fitting our assumptions for such geometry. Instead, the frequency-dependent current statistics have been measured experimentally for a system consisting of two-terminal quantum dot [25] with normal leads. Our formalism is flexible enough to describe the experimentally studied system. Thus in the following we shall compare the calculated frequency dependence of the Fano factors with experimental data [25] obtained in the large bias limit.

The experimentally investigated single electron transistor [25] consisted of the interacting quantum dot tunnel coupled to two normal electrodes. The authors [25] have studied the frequency dependence of the second and third cumulants of the currents. In the Coulomb blockade regime the individual charge transport events were measured *via* the quantum point contact placed near the quantum dot. The obtained current-current correlation function clearly shows the characteristic frequency dependence with a single correlation time.

Repeating the calculations for the quantum dot asymmetrically coupled to two normal electrodes we find the frequency-dependent Fano factor

$$F_R^N(\omega) = F_L^N(\omega) = 1 - \frac{2\Gamma_L\Gamma_R}{(\Gamma_L + \Gamma_R)^2 + \omega^2}, \quad (39)$$

for the large bias processes, when the electrons tunnel in one direction only. The corresponding cross-correlation factor reads (up to the sign, as elsewhere here we defined the cross-correlations with a minus sign)

$$F_{LR}^N(\omega) \equiv \frac{S_{LR}^N(\omega)}{2eJ} = \frac{\Gamma_L^2 + \Gamma_R^2}{(\Gamma_L + \Gamma_R)^2 + \omega^2}. \quad (40)$$



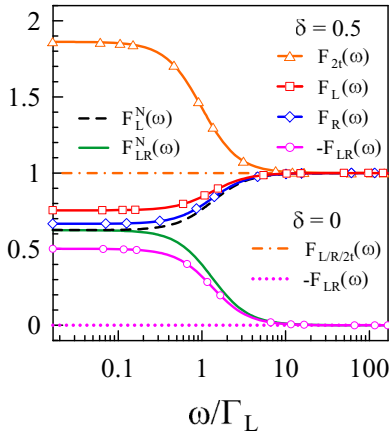


FIG. 5. The frequency-dependent Fano factors  $F_L(\omega)$  [ $F_R(\omega)$ ] of L-QD [QD-R] junction and  $F_{LR}(\omega) = S_{LR}(\omega)/2e\sqrt{|J_L J_R|}$  in three-terminal setup with the proximized quantum dot for the large bias voltage (see the Supplemental Material [68]). The Fano factors  $F_{2t}(\omega)$  [see Eq. (21)] of N-QD-S system are compared to  $F_L^N(\omega)$  and  $F_{LR}^N(\omega)$  of N-QD-N device, which has been investigated in Ref. [25]. For the proximized dot in the three-terminal setup our calculations have been performed using  $\Gamma_L = 3\Gamma_R = 0.006$ ,  $\Gamma_S = 0.2$ ,  $k_B T = 0.01$ , and  $\delta = \{0, 0.5\}$ , while for the dot hybridized with two normal electrodes we assumed  $\epsilon_1 = 0$  ( $U = 1$ ).

In the experiment the couplings were strongly asymmetric with  $\Gamma_L \approx 3\Gamma_R$  and the data, shown in Fig. 1(d) of the experimental paper [25], clearly feature single relaxation rate  $1/\tau_c = \Gamma_L + \Gamma_R$ . The experimental data essentially overlap the theoretical curves marked as  $F_L^N(\omega)$  and  $F_{LR}^N(\omega)$  in Fig. 5. This figure not only illustrates the frequency dependence of the factors (39) and (40), but also shows the corresponding frequency-dependent Fano factors of our two- and three-terminal proximized quantum dot. For the latter system we have defined these frequency-dependent factors as  $F_L(\omega) = S_{LL}(\omega)/2eJ_L$ ,  $F_R(\omega) = S_{RR}(\omega)/2eJ_R$  and  $F_{LR}(\omega) = S_{LR}(\omega)/2e\sqrt{|J_L J_R|}$  (see the Supplemental Material [68]) for two values of  $\delta = \{0, 0.5\}$  as indicated. In the three-terminal hybrid system the largest effect of the superconducting electrode (superconducting correlation) is seen for the electron-hole symmetry point ( $\delta = 0$ ). As  $\delta$  increases, the effect of the superconducting electrode clearly diminishes, while for the N-QD-S system the effect increases with  $\delta$ . The largest discrepancies between the two- or three-terminal hybrid and the normal (two-terminal) system occur for the low frequencies. If the hybrid system is close to the charge degeneracy point  $\delta \approx 0$  the contribution to  $S_{LR}(\omega)$  identically vanishes as also does the frequency-dependent part of  $F_L(\omega)$  and  $F_{2t}(\omega)$ , so it attains the form of Schottky noise with  $F_L = F_{2t} = 1$  independently of frequency. In Fig. 5 we also show the comparison of the frequency-dependent Fano factors for two normal terminals contacting the quantum dot when the Coulomb blockade is expected to play an important role with those of the three-terminal proximized dot as well as N-QD-S system. One can see that the Andreev scattering makes all frequency-dependent Fano factors to attain different values for  $\omega \rightarrow 0$ . This is related to charge nonconserving processes in individual normal electrodes. For  $\delta = 2$  (not shown) the

frequency-dependent Fano factors for the three-terminal dot with the superconducting electrode nearly coincide with those obtained for the system without proximity effect. This is traced back to the weak mixing of the empty and doubly occupied states for values of  $\delta \gg \Gamma_S$ .

On the other hand for N-QD-S system the frequency-dependent Fano factor  $F_{2t}(\omega)$  for large  $\delta$  approaches 2, which clearly indicates that the Cooper pairs tunneling is a Poissonian process. One can also easily check that with increasing asymmetry between  $\Gamma_L$  and  $\Gamma_R$  (i.e., with decrease of  $\Gamma_R$ ) one can observe that  $F_L(\omega)$  grows from the sub-Poissonian to the super-Poissonian values, and in the limit  $\Gamma_R \rightarrow 0$  one finds  $F_L(\omega) = F_{2t}(\omega)$ .

#### IV. SUMMARY OF MAIN FINDINGS

We have studied the charge current fluctuations for three-terminal hybrid system, comprising the QD sandwiched between two metallic leads and strongly coupled to superconductor. Using the generation-recombination approach [59,60] we have considered electron and hole tunneling through available subgap channels (in-gap bound states) of such proximized QD. In particular, we have addressed mutual relationship between the single electron transport (ET) and the Andreev (electron to hole) scattering caused by the local (DAR) and nonlocal (CAR) mechanisms. We have determined the currents and identified their components originating from transport through the specific bound states. We have analyzed the current-current correlation functions and performed their spectral decompositions, getting insight into the local and nonlocal fluctuations responsible for suppression or enhancement of the current noise. We have done numerical computations, focusing on the small and large bias voltages that activate either two or four in-gap Andreev levels in the transport window, respectively.

Assuming the symmetric couplings  $\Gamma_R = \Gamma_L$  and symmetric bias  $V_L = V/2 = -V_R$  we have found that single ET processes play important role in the local current-current correlation  $S_{LL}$ , leading to reduction of the shot noise to the sub-Poissonian regime with the zero-frequency Fano factor  $F_L < 1$ . Deviation from the Poissonian noise is caused by the dynamical (frequency-dependent) part of the current correlations. Its intrachannel components (tunneling processes through the same Andreev bound state) bring always the negative contribution, manifesting the antibunching behavior. On the other hand, the interchannel components can bring positive contribution. For small bias there appear positive correlations between the electrons and holes, indicating that the currents to the same normal lead originate from the direct Andreev reflection (DAR) processes. In such a situation the intra- and interchannel components describe the charge fluctuations with the same relaxation rate. On the other hand, for large bias, we observe two different charge fluctuation processes: one with the large relaxation rate  $1/\tau_{rel}^{ch} = 4\Gamma_L$  and another with the small relaxation rate  $1/\tau_{rel}^{pol} = 2\Gamma_L$ , respectively. Since in the symmetric case the charge is not accumulated on the Andreev bound states, the current correlation functions reveal a clear contribution from the charge and polarization fluctuations. The intrachannel correlations show only the negative component, corresponding to the

high-frequency charge relaxation, whereas the interchannel correlations have both the frequency terms. DAR processes are well manifested in the interchannel functions  $S_{LL}^{+,+}(\omega)$  and  $S_{LL}^{+,-}(\omega)$  [see Eq. (26)] with both positive frequency-dependent contributions. We noticed a somewhat intriguing behavior in charge fluctuations, where the intra- and interchannel correlation components compensate each other. For this reason the correlation function  $S_{LL}(\omega)$  for the total current has the frequency-dependent contribution, originating solely from the polarization fluctuations.

To emphasize the role of ET processes we have contrasted our results with those obtained for the two-terminal N-QD-S case, where the crossed Andreev reflection (CAR) processes are absent. Under such circumstances the bunching effect is well seen in the electron-hole correlation functions, implying the super-Poissonian noise with the zero-frequency Fano factor  $F_{2f} > 1$ . Our studies provide in-depth information about the dynamics of various internal charging processes. In particular, we can see relationship between the low-frequency polarization fluctuations and the high-frequency charge fluctuations in all components of the current correlation functions. This substantially extends the previous studies by Droste [45] and Braggio [44].

For the three-terminal heterostructure we have also inspected the nonlocal correlations between currents flowing through the left and the right tunnel junctions to metallic electrodes. The corresponding cross-correlation function  $S_{LR}$  exhibits a nontrivial interplay between the CAR and ET processes. For various gate voltages (arbitrary detuning  $\delta$  from the half-filled QD) we have found the negative values of  $S_{LR}$ , which indicates antibunching of the tunneling events typical for multiterminal normal systems (see e.g., Ref. [20]). Although the ET processes play the dominant role, the nonlocal CAR processes are important, especially near the electron-hole symmetry point,  $|\delta| \rightarrow 0$ , where  $S_{LR} \rightarrow 0$ . Enhancement of the shot noise originates from activation of the interchannel fluctuations between electron and holes. In the case of small bias this is due to the correlation function  $S_{LR}^{+,-,+}(\omega)$  [Eq. (19)] contributed by electrons and holes from different leads, which could be related to the CAR processes. For the large bias the correlation functions  $S_{LR}^{+,-,+}(\omega)$  and  $S_{LR}^{+,-,-}(\omega)$  [Eq. (38)], where the low-frequency polarization fluctuations are positive, become more relevant.

## V. CONCLUSIONS AND OUTLOOK

Our theoretical investigation of the quantum dot embedded into three-terminal heterostructure is quite universal, and it yields proper expressions for the charge fluctuations and the frequency-dependent Fano factors describing the statistical properties of the two-terminal N-QD-S and N-QD-N systems. Quantitative agreement of the present results with experimental data obtained recently for N-QD-N setup [25] and satisfactory agreement with the previous theoretical work on N-QD-S system [45] gives confidence that our method would be able to correctly describe the statistical correlations of the currents in hybrid systems with one superconducting and one or two normal electrodes. We thus hope that present analysis of the statistical properties of currents could stimulate further (experimental and theoretical) activities for this interesting

geometry. In particular, our predictions can be verified experimentally in the system similar to that used already by Ubbelohde *et al.* [25].

There is plenty of room for extending our studies in other directions as well. For instance, the auto- and cross-correlation have been discussed for the proximized QD coupled to magnetic electrodes in the Cooper pair splitter (CPS) configuration [49,50]. Such considerations, however, have been limited mostly to the zero-frequency case. It has to be mentioned that we are not considering the capacitive effects, which can be of importance in particular experiments and affect the frequency dependence of correlation functions. Our method, suitable for frequency-dependent current-current correlations, seems to give a broader insight into the dynamical processes of the Cooper pair formation (or splitting) in such devices [69]. Influence of the short-time fluctuations on efficiency of the Cooper pair entanglement might be crucial for future application of the CPS e.g., to quantum computation and/or communication. Furthermore, it has been recently observed, that the high-frequency cutoff completely washes out the emission noise related to the Kondo resonance [70]. It would be hence challenging to check whether such behavior can be overcome in the correlated quantum dots proximized to superconductors, where the subgap Kondo peak is expected to be substantially broadened upon approaching the doublet-singlet quantum phase transition [71,72].

Another interesting perspective would be possible in nanostructures, where the superconducting lead is in a topologically nontrivial phase hosting the Majorana boundary modes. Some authors [73] have pointed out that nonlocal nature of these zero-energy modes could be manifested by the strong cross-correlations detectable in the shot noise measurements. Leakage of these boundary modes onto side-attached quantum dots has been also proposed as a suitable tool for unambiguous recognition of the Majorana zero-energy quasiparticles from their trivial (finite-energy) counterparts [74,75].

Furthermore, three-terminal junctions with the quantum dot sandwiched between the topologically nontrivial superconducting nanowires could induce the giant shot noise [76]. Other setup, with the topological superconducting island coupled to three normal-conducting leads, has been recently proposed [77] for efficient protocol to test nonlocality of the Majorana bound states through the current shot-noise correlations, where the zero-frequency Fano factor could detect the exotic (non-Abelian) character of the Majorana quasiparticles [78]. These examples show a rich variety of heterostructures, where our study can be potentially extended.

## ACKNOWLEDGMENTS

This research was financed by the National Science Centre (Poland) under the Projects No. 2016/21/B/ST3/02160 (B.R.B., G.M.) and No. 2017/27/B/ST3/01911 (T.D., K.I.W.).

## APPENDIX: MASTER EQUATION APPROACH

In the weak coupling limit  $\Gamma_{L(R)} \ll k_B T$ ,  $\Gamma_S$  transport properties of our nanostructure are dominated by a sequential tunneling processes through the proximized QD. The currents

can be determined by solving the master equation

$$\dot{\mathbf{p}}(t) = \mathbf{M} \mathbf{p}(t) \quad (\text{A1})$$

with the probabilities  $\mathbf{p}(t) = (p_1(t), p_-(t), p_+(t))^T$  referring to the single-electron occupancy of QD  $p_1(t) = p_\uparrow(t) + p_\downarrow(t)$  and probabilities of the BCS-type configurations  $|-\rangle$  and  $|+\rangle$  denoted by  $p_-(t)$  and  $p_+(t)$ , respectively. Probability conservation implies the constraint  $p_1(t) + p_-(t) + p_+(t) \equiv 1$ .

The evolution matrix  $\mathbf{M}$  has in our problem the following structure:

$$\mathbf{M} = \begin{pmatrix} -M_{21} - M_{31} & M_{12} & M_{13} \\ M_{21} & -M_{12} & 0 \\ M_{31} & 0 & -M_{13} \end{pmatrix}, \quad (\text{A2})$$

where  $M_{12} = 2 \sum_{\alpha=L,R} (\Gamma_{\alpha+}^{+-} + \Gamma_{\alpha-}^{+-})$ ,  $M_{13} = 2 \sum_{\alpha=L,R} (\Gamma_{\alpha+}^{++} + \Gamma_{\alpha-}^{++})$ ,  $M_{21} = \sum_{\alpha=L,R} (\Gamma_{\alpha+}^{+-} + \Gamma_{\alpha-}^{+-})$ , and  $M_{31} = \sum_{\alpha=L,R} (\Gamma_{\alpha+}^{++} + \Gamma_{\alpha-}^{++})$ . We have introduced here the effective transition rates  $\Gamma_{\alpha\pm}^i$  describing tunneling processes to/from the QD (+/-) through  $\alpha$ th junction and engaging the Andreev bound states  $i \in \{ABS\} \equiv \{++, +-, -+, --\}$ ; see Fig. 1. The tunneling rates describe transfer of one electron or hole between the singly occupied states and the singlet subspace. In particular,  $\Gamma_{\alpha\pm}^{++} = \alpha_{\pm}^2 \Gamma_{\alpha} f(\pm E_A^{++} \mp \mu_{\alpha})$ ,  $\Gamma_{\alpha\pm}^{+-} = \alpha_{\pm}^2 \Gamma_{\alpha} f(\pm E_A^{+-} \mp \mu_{\alpha})$ ,  $\Gamma_{\alpha\pm}^{-+} = \alpha_{\pm}^2 \Gamma_{\alpha} f(\pm E_A^{-+} \mp \mu_{\alpha})$ , and  $\Gamma_{\alpha\pm}^{--} = \alpha_{\pm}^2 \Gamma_{\alpha} f(\pm E_A^{--} \mp \mu_{\alpha})$ , where  $f(E) = [1 + \exp(E/k_B T)]^{-1}$  is the Fermi-Dirac distribution function. In the case of positive Andreev bound states,  $E_A^i > \mu_S$ , the

tunneling rate  $\Gamma_{\alpha\pm}^i$  describes an electron transfer, whereas for  $E_A^i < \mu_S$  the charge current is contributed by holes. The chemical potential of the superconducting electrode is denoted as  $\mu_S$  and its value is assumed to be  $\mu_S = 0$  throughout.

The charge current flowing from  $\alpha$ th lead can be expressed in the stationary limit as  $J_{\alpha} = \sum_{i \in \{ABS\}} J_{\alpha}^i$ , where the contributions from the Andreev bound states are given by

$$J_{\alpha}^{++} \equiv I_{\alpha+}^{++} - I_{\alpha-}^{++} = e(\Gamma_{\alpha+}^{++} p_1^0 - 2\Gamma_{\alpha-}^{++} p_+^0), \quad (\text{A3})$$

$$J_{\alpha}^{+-} \equiv I_{\alpha+}^{+-} - I_{\alpha-}^{+-} = e(\Gamma_{\alpha+}^{+-} p_1^0 - 2\Gamma_{\alpha-}^{+-} p_-^0), \quad (\text{A4})$$

$$J_{\alpha}^{-+} \equiv I_{\alpha+}^{-+} - I_{\alpha-}^{-+} = -e(\Gamma_{\alpha-}^{-+} p_1^0 - 2\Gamma_{\alpha+}^{-+} p_-^0), \quad (\text{A5})$$

$$J_{\alpha}^{--} \equiv I_{\alpha+}^{--} - I_{\alpha-}^{--} = -e(\Gamma_{\alpha-}^{--} p_1^0 - 2\Gamma_{\alpha+}^{--} p_+^0). \quad (\text{A6})$$

Under stationary conditions the probability  $\mathbf{p}^0 = (p_1^0, p_-^0, p_+^0)^T$  can be determined, solving the equation  $\mathbf{M}\mathbf{p}^0 = \mathbf{0}$ . The currents  $J_{\alpha}^{++}$  and  $J_{\alpha}^{+-}$  are contributed by electrons (“e”), whereas  $J_{\alpha}^{-+}$  and  $J_{\alpha}^{--}$  by holes (“h”) via the corresponding Andreev bound states; see Fig. 1. One can notice that for  $|\delta| = 1$  the Andreev bound states  $E_A^{+-}$  and  $E_A^{-+}$  cross each other, signifying the quantum phase transition [58]. For large  $|\delta| > 1$  the currents  $J_{\alpha}^{+-}$  and  $J_{\alpha}^{-+}$  describe hence transport of holes and electrons, respectively. As far as the Copper pair current  $J_S$  is concerned (flowing from the QD to superconducting lead) it can be obtained from the Kirchoff’s law  $J_S = J_L + J_R$ .

- 
- [1] G. Benenti, G. Casati, K. Saito, and R. S. Whitney, *Phys. Rep.* **694**, 1 (2017).
- [2] S. De Franceschi, L. Kouwenhoven, C. Schönberger, and W. Wernsdorfer, *Nat. Nanotechnol.* **5**, 703 (2010).
- [3] W. G. van der Wiel, S. De Franceschi, J. M. Elzerman, T. Fujisawa, S. Tarucha, and L. P. Kouwenhoven, *Rev. Mod. Phys.* **75**, 1 (2003).
- [4] D. M. Zumbühl, C. M. Marcus, M. P. Hanson, and A. C. Gossard, *Phys. Rev. Lett.* **93**, 256801 (2004).
- [5] F. Mazza, S. Valentini, R. Bosisio, G. Benenti, V. Giovannetti, R. Fazio, and F. Taddei, *Phys. Rev. B* **91**, 245435 (2015).
- [6] B. Braunecker, P. Burset, and A. Levy Yeyati, *Phys. Rev. Lett.* **111**, 136806 (2013).
- [7] P. Zoller, Th. Beth, D. Binosi, R. Blatt, H. Briegel, D. Bruss, T. Calarco, J. I. Cirac, D. Deutsch, J. Eisert *et al.*, *Eur. Phys. J. D* **36**, 203 (2005).
- [8] A. Martín-Rodero and A. Levy-Yeyati, *Adv. Phys.* **60**, 899 (2011).
- [9] M. Eschrig, *Phys. Today* **64**, 43 (2011).
- [10] P. Recher, E. V. Sukhorukov, and D. Loss, *Phys. Rev. B* **63**, 165314 (2001).
- [11] S. Russo, M. Kroug, T. M. Klapwijk, and A. F. Morpurgo, *Phys. Rev. Lett.* **95**, 027002 (2005).
- [12] L. Hofstetter, S. Csonka, J. Nygård, and C. Schönberger, *Nature (London)* **461**, 960 (2009).
- [13] J. Schindele, A. Baumgartner, and C. Schönberger, *Phys. Rev. Lett.* **109**, 157002 (2012).
- [14] Y. Blanter and M. Büttiker, *Phys. Rep.* **336**, 1 (2000).
- [15] R. P. Feynman, R. B. Leighton, and M. Sands, *The Feynman Lectures*, Vol. 3 (Addison-Wesley, Reading, MA, 1965).
- [16] G. Iannaccone, G. Lombardi, M. Macucci, and B. Pellegrini, *Phys. Rev. Lett.* **80**, 1054 (1998); *Nanotechnology* **10**, 97 (1999).
- [17] B. R. Buřka, J. Martinek, G. Michařek, and J. Barnař, *Phys. Rev. B* **60**, 12246 (1999).
- [18] B. R. Buřka, *Phys. Rev. B* **62**, 1186 (2000).
- [19] G. Michařek and B. R. Buřka, *Eur. Phys. J. B* **28**, 121 (2002).
- [20] B. R. Buřka, *Phys. Rev. B* **77**, 165401 (2008).
- [21] G. Michařek and B. R. Buřka, *Phys. Rev. B* **80**, 035320 (2009).
- [22] B. Dong, X. L. Lei, and N. J. M. Horing, *Phys. Rev. B* **80**, 153305 (2009).
- [23] D. T. McClure, L. DiCarlo, Y. Zhang, H.-A. Engel, C. M. Marcus, M. P. Hanson, and A. C. Gossard, *Phys. Rev. Lett.* **98**, 056801 (2007).
- [24] Y. Zhang, L. DiCarlo, D. T. McClure, M. Yamamoto, S. Tarucha, C. M. Marcus, M. P. Hanson, and A. C. Gossard, *Phys. Rev. Lett.* **99**, 036603 (2007).
- [25] N. Ubbelohde, C. Fricke, C. Flindt, F. Hohls, and R. J. Haug, *Nat. Commun.* **3**, 612 (2012).
- [26] J. Börlin, W. Belzig, and C. Bruder, *Phys. Rev. Lett.* **88**, 197001 (2002).
- [27] J. P. Morten, D. Huertas-Hernando, W. Belzig, and A. Brataas, *Phys. Rev. B* **78**, 224515 (2008).
- [28] M. P. Anantram and S. Datta, *Phys. Rev. B* **53**, 16390 (1996).
- [29] J. Torrès and T. Martin, *Eur. Phys. J. B* **12**, 319 (1999).

- [30] G. Bignon, M. Houzet, F. Pistolesi, and F. W. J. Hekking, *Europhys. Lett.* **67**, 110 (2004).
- [31] A. Freyn, M. Flöser, and R. Mélin, *Phys. Rev. B* **82**, 014510 (2010).
- [32] J. Wei and V. Chandrasekhar, *Nat. Phys.* **6**, 494 (2010).
- [33] M. Flöser, D. Feinberg, and R. Mélin, *Phys. Rev. B* **88**, 094517 (2013).
- [34] V. F. Maisi, D. Kambly, C. Flindt, and J. P. Pekola, *Phys. Rev. Lett.* **112**, 036801 (2014).
- [35] M. Albert, D. Chevallier, and P. Devillard, *Physica E* **76**, 209 (2016).
- [36] J. A. Celis Gil, S. Gomez P., W. J. Herrera, *Solid State Commun.* **258**, 25 (2017).
- [37] D. S. Golubev and A. D. Zaikin, *Phys. Rev. B* **99**, 144504 (2019).
- [38] S. Valentini, M. Governale, R. Fazio, and F. Taddei, *Physica E* **75**, 15 (2016).
- [39] A. Komnik, *Phys. Rev. B* **93**, 125117 (2016).
- [40] H.-K. Zhao, *Phys. Lett. A* **299**, 262 (2002).
- [41] A. O. Gogolin and A. Komnik, *Phys. Rev. B* **73**, 195301 (2006).
- [42] P. Zhang and Y.-X. Li, *J. Phys.: Condens. Matter* **21**, 095602 (2009).
- [43] H. Soller and A. Komnik, *Eur. Phys. J. D* **63**, 3 (2011); *Physica E* **44**, 425 (2011).
- [44] A. Braggio, M. Governale, M. G. Pala, and J. König, *Solid State Commun.* **151**, 155 (2011).
- [45] S. Droste, J. Splettstoesser, and M. Governale, *Phys. Rev. B* **91**, 125401 (2015).
- [46] B. Dong, G. H. Ding, and X. L. Lei, *Phys. Rev. B* **95**, 035409 (2017).
- [47] R. Avriller and F. Pistolesi, *Phys. Rev. Lett.* **114**, 037003 (2015).
- [48] A. Das, Y. Ronen, M. Heiblum, D. Mahalu, A. V. Kretinin, and H. Shtrikman, *Nat. Commun.* **3**, 1165 (2012).
- [49] S. Weiss and J. König, *Phys. Rev. B* **96**, 064529 (2017).
- [50] P. Trocha and K. Wrzeźniewski, *J. Phys.: Condens. Matter* **30**, 305303 (2018).
- [51] N. Walldorf, C. Padurariu, A.-P. Jauho, and C. Flindt, *Phys. Rev. Lett.* **120**, 087701 (2018).
- [52] P. Stegmann and J. König, *Phys. Rev. B* **94**, 125433 (2016).
- [53] L. Rajabi, Ch. Pörtl, and M. Governale, *Phys. Rev. Lett.* **111**, 067002 (2013) and Supplementary information.
- [54] G. Michałek, B. R. Bułka, T. Domański, and K. I. Wysokiński, *Acta Phys. Pol. A* **133**, 391 (2018).
- [55] J. Gramich, A. Baumgartner, and C. Schönenberger, *Phys. Rev. B* **96**, 195418 (2017).
- [56] E. Vecino, A. Martín-Rodero, and A. Levy Yeyati, *Phys. Rev. B* **68**, 035105 (2003).
- [57] K. I. Wysokiński, *J. Phys.: Condens. Matter* **24**, 335303 (2012).
- [58] J. Bauer, A. Oguri, and A. C. Hewson, *J. Phys.: Condens. Matter* **19**, 486211 (2007).
- [59] K. M. van Vliet and J. R. Fasset, in *Fluctuation Phenomena in Solids*, edited by R. E. Burgess (Academic Press, New York, 1965), p. 267.
- [60] A. N. Korotkov, *Phys. Rev. B* **49**, 10381 (1994).
- [61] G. Michałek, B. R. Bułka, T. Domański, and K. I. Wysokiński, *Phys. Rev. B* **88**, 155425 (2013).
- [62] G. Michałek, T. Domański, B. R. Bułka, and K. I. Wysokiński, *Sci. Rep.* **5**, 14572 (2015).
- [63] G. Michałek, M. Urbaniak, B. R. Bułka, T. Domański, and K. I. Wysokiński, *Phys. Rev. B* **93**, 235440 (2016).
- [64] S. Swain, *J. Phys. A: Math. Gen.* **14**, 2577 (1981).
- [65] H.-P. Breuer and F. Petruccione, *The Theory of Open Quantum Systems* (Oxford University Press, Oxford, 2002).
- [66] A. Crépieux, S. Sahoo, T. Q. Duong, R. Zamoum, and M. Lavagna, *Phys. Rev. Lett.* **120**, 107702 (2018).
- [67] D. Marcos, C. Emary, T. Brandes, and R. Aguado, *New J. Phys.* **12**, 123009 (2010).
- [68] See Supplemental Material at <http://link.aps.org/supplemental/10.1103/PhysRevB.101.235402> for the details concerning frequency-dependent noise of the two terminal N-QD-S system as well as three terminal system with arbitrary couplings of the quantum dot to two normal electrodes.
- [69] G. Michałek *et al.* (unpublished).
- [70] R. Delagrè, J. Basset, H. Bouchiat, and R. Deblock, *Phys. Rev. B* **97**, 041412(R) (2018).
- [71] R. Žitko, J. S. Lim, R. López, and R. Aguado, *Phys. Rev. B* **91**, 045441 (2015).
- [72] T. Domański, I. Weymann, M. Barańska, and G. Górski, *Sci. Rep.* **6**, 23336 (2016).
- [73] P. Wang, Y. Cao, M. Gong, G. Xiong, and X.-Q. Li, *Europhys. Lett.* **103**, 57016 (2013).
- [74] D. E. Liu, M. Cheng, and R. M. Lutchyn, *Phys. Rev. B* **91**, 081405(R) (2015).
- [75] M. Hell, K. Flensberg, and M. Leijnse, *Phys. Rev. B* **97**, 161401(R) (2018).
- [76] T. Jonckheere, J. Rech, A. Zazunov, R. Egger, A. L. Yeyati, and T. Martin, *Phys. Rev. Lett.* **122**, 097003 (2019).
- [77] J. Manousakis, C. Wille, A. Altland, R. Egger, K. Flensberg, and F. Hassler, *Phys. Rev. Lett.* **124**, 096801 (2020).
- [78] H.-Z. Lu, *Physics* **13**, 30 (2020).